

# Metabolic remodeling of the human red blood cell membrane measured by quantitative phase microscopy

YongKeun Park<sup>\*a</sup>, Catherine Best<sup>b</sup>, Thorsten Auth<sup>c</sup>, Nir S. Gov<sup>d</sup>, Samuel Safran<sup>e</sup>,  
and Gabriel Popescu<sup>f</sup>

<sup>a</sup>Department of Physics, KAIST, Daejeon, Republic of Korea 305-701 <sup>b</sup>College of Medicine and  
<sup>f</sup>Department of Electrical and Computer Engineering, UIUC, IL, USA 61801, <sup>c</sup>Forschungszentrum  
Jülich, Institute for Complex Systems, 52425 Jülich, Germany, <sup>d</sup>Department of Chemical Physics,  
and <sup>e</sup>Department of Materials and Interfaces, Weizmann Institute of Science, Rehovot, Israel 76100.

\*yk.park@kaist.ac.kr; phone 82 42 350-2514; bmokaist.wordpress.com

## ABSTRACT

We have quantitatively and systemically measured the morphologies and dynamics of fluctuations in human RBC membranes using a full-field laser interferometry technique that accurately measures dynamic membrane fluctuations. We present conclusive evidence that the presence of adenosine 5'-triphosphate (ATP) facilitates nonequilibrium dynamic fluctuations in the RBC membrane and that these fluctuations are highly correlated with specific regions in the biconcave shape of RBCs. Spatial analysis reveals that these nonequilibrium membrane fluctuations are enhanced at the scale of the spectrin mesh size. Our results indicate the presence of dynamic remodeling in the RBC membrane cortex powered by ATP, which results in nonequilibrium membrane fluctuations. (This conference proceeding paper is primary based on our recent publication - please refer to YK Park et al., *Proc. Nat. Acad. Sci.*, 107, 1289 (2010) for details.)

**Keywords:** quantitative phase microscopy, red blood cell, membrane dynamics, biophysics, ATP

## 1. INTRODUCTION

As human red blood cells (RBCs) circulate in capillaries and pass small holes in the spleen, they undergo repeated severe deformations. The RBC membrane has remarkable deformability and stability that are governed by the structure of red blood cell membrane cortex, and the coupling and interactions between the bilayer and the cortical spectrin network [1]. This composite membrane is dramatically soft and elastic, and thus exhibits membrane fluctuations, with amplitudes of the order of tens of nanometers. These fluctuations have been studied to better understand the mechanical properties of the complex RBC membrane [2-12].

While fluctuations of the RBC membrane have been observed for decades, their physical origin (e.g. whether they originate from thermal or from active processes) has remained uncertain. Quantitative measurements of the membrane fluctuations are crucial for understanding the interactions between the lipid bilayer and the cytoskeleton network. First observed a century ago [13], their origin is generally believed to stem from thermal forces [2]. Different interference-microscopic techniques have been employed to study membrane fluctuations and to extract mechanical properties assuming Brownian dynamics [3, 5]. In contrast, using a technique to measure local fluctuations of RBC membranes, a correlation between the ATP concentration and the fluctuation amplitude has been reported [10, 14]. A recent experimental work in which only edge shapes of RBCs were probed showed no relation between ATP depletion and membrane fluctuations [15]. Theoretically RBC membrane fluctuations were traditionally studied using models of thermally driven equilibrium systems [2, 3]. A theoretical model [16], validated by simulation [17], showed that local breaking and reforming of the spectrin network can result in enhanced fluctuations.

We present direct, full-field, and quantitative measurements of ATP effects on RBC membrane morphology and fluctuations through Diffraction Phase Microscopy [18, 19]. By extracting the optical path-length shifts produced across the cell, we measured the cell thickness with nanometer sensitivity and millisecond temporal resolution. RBC samples were prepared under four different conditions: healthy RBCs, irreversibly ATP-depleted RBCs, metabolically ATP-depleted RBCs, and RBCs with recovered ATP concentration. After collection, the group of healthy RBCs was

minimally prepared. For RBCs in the irreversibly ATP-depleted group, the cytoplasmic pool of ATP was depleted by inosine and iodoacetamide. For the metabolically-depleted ATP group, healthy RBCs were incubated in a glucose-free medium for 24 hours. For RBCs in the ATP repleted group, cytoplasmic ATP was first metabolically depleted, and then regenerated through the addition of D-glucose.

## 2. METHODS

### 2.1 Sample preparation

Human RBCs were extracted from a healthy volunteer and were collected in vacutainer tubes containing an anticoagulant (ethylenediaminetetraacetic acid). The tubes were immediately centrifuged at 2000 g for 10 min at 10°C to separate RBCs and plasma. The RBCs were then washed three times with Phosphate Buffered Saline (PBS). After washing, the RBCs were resuspended in PBS to approximately 20% hematocrit (Ht).

We prepared six different groups of RBCs in this study following the standard protocol[20]: (a) RBCs with physiological levels of ATP (no additional treatment after resuspending RBC samples), (b) metabolically ATP-depleted RBCs, (c) irreversibly ATP-depleted RBCs (with high dose of inosine and iodoacetamide), (d) irreversibly ATP-depleted RBCs (with low dose of inosine and iodoacetamide), (e) ATP-repleted RBCs after metabolic ATP depletion, and (f) an osmotic control group. For metabolically ATP-depleted RBCs, the RBCs were incubated in glucose-free PBS for 24 h at 37°C. We prepared two different sub-groups for the irreversible ATP depletion (high dose and low dose). For the first irreversibly ATP-depleted group (high dose depletion group), the RBCs were incubated without glucose in the presence of 10 mM inosine (A3221, Sigma-Aldrich) and 6 mM iodoacetamide (I1024, Sigma-Aldrich) for 2 h at 20°C. For the second group of irreversibly ATP-depleted RBCs (low-dose depletion group), the RBCs were treated the same as the high-dose ATP-depleted group except that 3 mM inosine and 1 mM iodoacetamide was used. Inosine consumes ATP and iodoacetamide blocks ATP production by inhibiting glyceraldehydes-3phosdehydrogenase. For the ATP-reintroduced RBCs, 10 mM of D-glucose was added to the RBC suspension in the metabolically ATP-depleted group. For the osmotic control group, 10 mM L-glucose was added to a RBC suspension in the metabolically ATP-depleted group. This study was approved by the Massachusetts Institute of Technology's Committee on the Use of Humans as Experimental Subjects.

### 2.2 Diffraction Phase Microscopy

The 10  $\mu$ L of RBC suspension was introduced between two glass slides and the dynamic membrane fluctuations were measured using Diffraction Phase Microscopy (DPM) [19, 21]. DPM is a highly stable and sensitive quantitative phase microscopy, which employs laser interferometry in a common path geometry and thus provides full-field quantitative phase images of biological samples with unprecedented optical path length stability. An Ar<sup>2+</sup> laser ( $\lambda=514$  nm) was used as illumination source. An inverted microscope (IX71, Olympus American Inc.) was equipped with a 40X objective (0.65 NA), which facilitates a diffraction-limited transverse resolution of 400 nm. With the additional relay optics, the overall magnification of the system was 200 $\times$ . EMCCD (Photonmax512B, Princeton Instruments) was used to image interferograms. The instantaneous cell thickness map is obtained as  $h(x,y,t)=\lambda/(2\pi\Delta n)\cdot\phi(x,y,t)$ , with  $\phi$  the quantitative phase image measured by DPM. The refractive index contrast  $\Delta n$  between the RBC and the surrounding medium is mainly attributed to Hb in RBC cytosol. The values for  $\Delta n$  were used from the previous report [21]. The DPM optical path length stability is 2.4 mrad, which corresponds to a 3.3 nm displacement of the RBC membrane [18]. Recently, DPM has been extended for measuring refractive index in the deep ultraviolet range and the dispersion phase image [22, 23]. The details for the DPM instrumentation and analysis can be found elsewhere [18, 19, 24].

### 2.3 Non-Gaussian parameter

The non-Gaussian parameter,  $\kappa$ , is defined by the second and fourth moments of the membrane height displacement. First, the displacement maps of membrane fluctuations,  $\Delta h(x,y,t)$ , are decomposed into Fourier modes  $\Delta h(q,\Delta t)$ ;  $\Delta t$  is the lag time,  $q=2\pi/\Lambda$  the spatial frequencies, and  $\Lambda$  a spatial distance.

$\kappa$  is then calculated from the second and fourth moments of the membrane height displacement,

$$\kappa = \frac{\langle |h(q,\Delta t) - h(q,0)|^4 \rangle}{\langle |h(q,\Delta t) - h(q,0)|^2 \rangle^2} = \frac{\langle |h_q|^4 \rangle}{\langle |h_q|^2 \rangle^2} . \quad \text{When } h_q \text{ is defined as } h_q = a_q + ib_q ,$$

$$\langle a_q^2 \rangle = \langle b_q^2 \rangle = \frac{1}{2} \langle |h_q|^2 \rangle \quad \text{and} \quad \langle a_q^4 \rangle = \langle b_q^4 \rangle = \frac{3}{8} \langle |h_q|^4 \rangle \quad (\text{see Ref. [25]}). \quad \text{For } \Delta t \text{ longer than the relaxation time of the}$$

membrane, the difference of two normally distributed variables is also normally distributed,  $\kappa = \frac{\langle |h_q|^4 \rangle}{\langle |h_q|^2 \rangle^2} = \frac{8}{3} \cdot \frac{3}{4} = 2$ .

## 2.4 Statistical analysis

$P$  values are calculated by two-tailed Mann-Whitney rank sum tests comparing the RMS fluctuations between various test conditions. All the numbers follow the  $\pm$  sign in the text is a standard deviation.

# 3. RESULTS AND DISCUSSIONS

## 3.1 ATP enhances the dynamic fluctuation in RBC membrane

We first address the effects of ATP on the morphologies of RBC membranes. From the measured cell thickness profiles at a given time  $t$ ,  $h(x,y,t)$ , we calculated (Figs. 1a-d) time-averaged heights  $\langle h(x,y,t) \rangle$  and observed the characteristic biconcave shape for healthy RBCs. When ATP was depleted, for both the irreversibly and the metabolically depleted groups, we observed loss of biconcave shape and echinocyte shape transformation. Reintroducing ATP resulted in the recovery of biconcave shape. This shows that ATP is crucial to maintaining biconcave shape of RBCs [26].

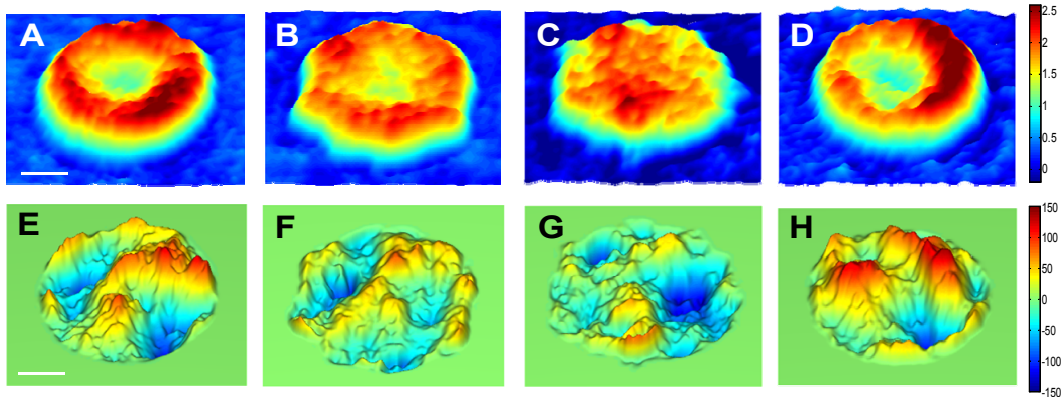


Figure 1. Topography of a healthy RBC (A), of an ATP-depleted RBC (irreversible -ATP group) (B), of an ATP-depleted RBC (metabolic -ATP group) (C), and of a RBC with recovered ATP level (+ATP group) (D), respectively. (E-H), Instantaneous displacement maps of membrane fluctuation in the Figs. 1a-d, respectively. The scale bar is 2  $\mu\text{m}$ . The colorbar scales are in  $\mu\text{m}$  and nm, respectively. Reprinted from Ref. [27]. Copyright (2010) National Academy of Sciences, USA

To probe dynamic membrane fluctuations, we analyzed the membrane displacement map by subtracting the averaged shape from the cell thickness map,  $\Delta h(x,y,t) = h(x,y,t) - \langle h(x,y,t) \rangle$  (Figs. 1e-h). Compared to healthy RBCs, the fluctuation amplitudes were decreased in both ATP-depleted groups. Reintroducing ATP increased the fluctuation amplitudes to healthy RBC levels. We calculated the root mean squared (RMS) displacement of membrane fluctuations,  $\langle \Delta h^2 \rangle^{1/2}$ , which covers the entire cell area for 2 s at 120 frame/s. The RMS displacement of healthy RBCs is  $41.5 \pm 5.7$  nm. Fluctuations significantly decreased to  $32.0 \pm 7.8$  nm and  $33.4 \pm 8.7$  nm in both the irreversibly metabolically ATP-depleted groups, respectively. However, the fluctuations in the ATP repleted group returned to the level of healthy RBCs ( $48.4 \pm 10.2$  nm). This is in agreement with Refs. [10, 14].

### 3.2 Non equilibrium dynamic in membrane fluctuation

Although we thus showed that the membrane fluctuations indeed decrease in the absence of ATP, this result does not yet answer the question of whether ATP drives ‘active’ non-equilibrium dynamics or modifies membrane elastic properties. Of course, the two different situations can give rise to fundamentally different dynamics: (i) non-Gaussian out-of-equilibrium fluctuations and (ii) the equilibrium Gaussian statistics. We have calculated the non-Gaussian parameter,  $\kappa$ , for the membrane fluctuations (Figs. 2b-e). Theoretically,  $\kappa=2$  is expected for purely thermally driven Gaussian motion and  $\kappa>2$  might indicated non-equilibrium dynamics [25]. For healthy RBCs, the average value of  $\kappa$  was 2.8, which shows that membrane fluctuations contain non-equilibrium dynamic components particularly on short length and time scales ( $q>5$  rad/ $\mu\text{m}$  and  $\Delta t <0.5$  s). With depletion of ATP,  $\kappa$  decreased to 2, as expected in purely thermally-driven dynamics (the average values of  $\kappa$  were 2.06 and 2.19 for the irreversibly depleted and metabolically depleted ATP groups, respectively). Reintroducing ATP increased  $\kappa$  to healthy-RBC levels (average value  $\kappa =2.98$ ). Our data clearly proves that active, metabolic energy from ATP contributes an enhancement in RMS displacements by 44.9%. This measured value is lower than predicted by a theoretical model, where an increase of at least 100% was expected [25]. However, it can be explained by recognizing that the ATP effect is more significant at large  $q$ -values that are comparable with the size of the spectrin network [16]. For example, the ATP-mediated RMS displacement at  $q=17\pm0.5$  rad/ $\mu\text{m}$  showed an increase of 143% compared with the thermal components. Thus, in our overall assessment that includes all spatial frequencies, ATP enhancement is likely to be underestimated.

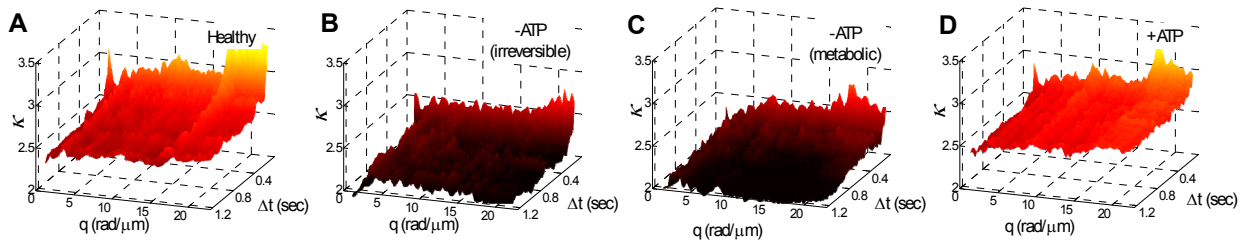


Figure 2. Averaged non-Gaussian parameter versus a lag time,  $\Delta t$ , and a spatial frequency,  $q$ , for membrane fluctuation: (A) healthy RBCs, (B) irreversible ATP-depleted RBCs, (C) metabolically ATP-depleted RBCs and (D) RBCs with recovered ATP level after metabolic depletion.  $N=40$  RBCs per each group. Reprinted from Ref. [27]. Copyright (2010) National Academy of Sciences, USA

### 3.3 Spatial distribution of membrane fluctuation

In order to study further spatial aspects of active motions, we analyzed the morphologies and fluctuations for RBCs in a polar coordinate system with its origin at cell center. Assuming cylindrical symmetry, the average height of the RBC membrane,  $\langle h(r) \rangle$ , and the membrane mean-squared displacements,  $\langle h^2(r) \rangle$ , are shown as functions of the radial distance,  $r$  (Figs. 3). In healthy RBCs, the membrane fluctuations are enhanced and strongly localized at the outer region, while both ATP depletion groups showed little variation in membrane fluctuations over the cell surface. Remarkably, reintroducing ATP restores not only the biconcave shape, but also enhanced fluctuations in the outer area. This is striking because continuum models predict stronger restoring force and decreased fluctuation amplitude in regions of high membrane curvature [28]. This result shows that active fluctuations are spatially inhomogeneous and correlated with the maintenance of the biconcave shape. It also rationalizes different mechanistic inferences reported in the literature from prior measurement of membrane fluctuations [14, 15, 29]. Probing the edge shape of RBCs alone does not capture ATP-dependent enhanced fluctuations [15] since they are localized on the outer cell and may not be significant only after 1 hour of ATP depletion. Dark-field microscopy, which qualitatively measures the averaged dynamics of RBC surface, could however measure ATP-dependence [14, 29].

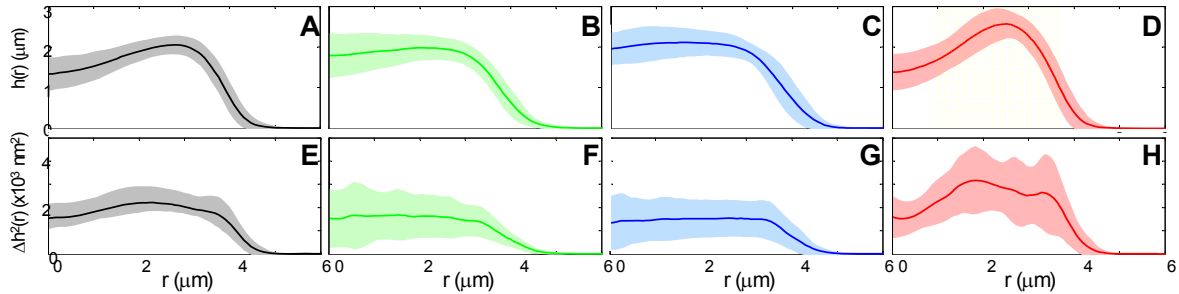


Figure 3. Averaged height as a function of the distance from the center of cells for healthy RBCs (A), for RBCs in the irreversibly ATP-depleted group (B), for RBCs in the metabolically ATP-depleted group (C), and for RBCs in which ATP was reintroduced to the metabolically ATP-depleted group (D), respectively. (E-H), Averaged squared height fluctuations as a function of the distance from the center of cells in Figs. 3a-d, respectively. Thick lines show the average value and the areas represent standard deviation for 40 RBCs. Reprinted from Ref. [27]. Copyright (2010) National Academy of Sciences, USA

### 3.4 Spatial harmonic dynamic in active membrane fluctuation

Other cytoskeleton models incorporating actin, microtubules, and motor proteins such as myosin have demonstrated active motion [30]. However, this cannot be the case for the ATP-enhanced fluctuations in RBC because motor proteins are absent here. Then, how can the RBC exhibit active dynamics? To address this question, we further analyzed the results in the context of RBC cytoskeletal structure. The non-Gaussian parameter,  $\kappa$ , at short time delays, was plotted as a function of spatial distance  $A=2\pi/q$  (Fig. 4a). Interestingly, in the presence of ATP,  $\kappa$  showed distinct peaks at specific distances ( $A=361, 512, 680, 860, \text{ and } 1030 \text{ nm}$ ); these peaks are equally spaced at  $167\pm 10 \text{ nm}$ . These results indicate that ATP-dependent enhanced fluctuations are correlated with the network structure of the underlying cytoskeleton. Considering the roughly hexagonal lattice of spectrin network, these peaks can be related to the dynamic remodeling of spectrin network by ATP. Possible elements responsible for this remodeling are the junctional complexes of the spectrin network which consist of a complex of six spectrin polymers joined by short actin segments and protein-4.1 (Fig. 4b). It was proposed that this ATP-induced remodeling takes the form of local associations and dissociations of spectrin filaments within the network or between the cytoskeleton and the lipid membrane [4, 16]. Both processes result in the formation of structural defects in the hexagonal network, of size  $\sim 2\Delta$ , where  $\Delta$  is a distance between neighboring junctions (Fig. 4c). This remodeling of the cytoskeletal attachment causes a local release of the cytoskeleton-induced membrane tension, and results in local bilayer deformation [4, 16]. The length-scale of this local, ATP-induced, bilayer deformation will therefore be in multiples of the junction spacing,  $2\Delta$ . From the data we find  $\Delta \sim 83.5\pm 5 \text{ nm}$ , which is in good agreement with the separation of the junctions complexes measured by electron microscopy [31]. In addition,  $\kappa$  at the short distance  $2\Delta$  was plotted as a function of a lag time (Fig. 4d), which shows longer temporal correlations in the presence of ATP.

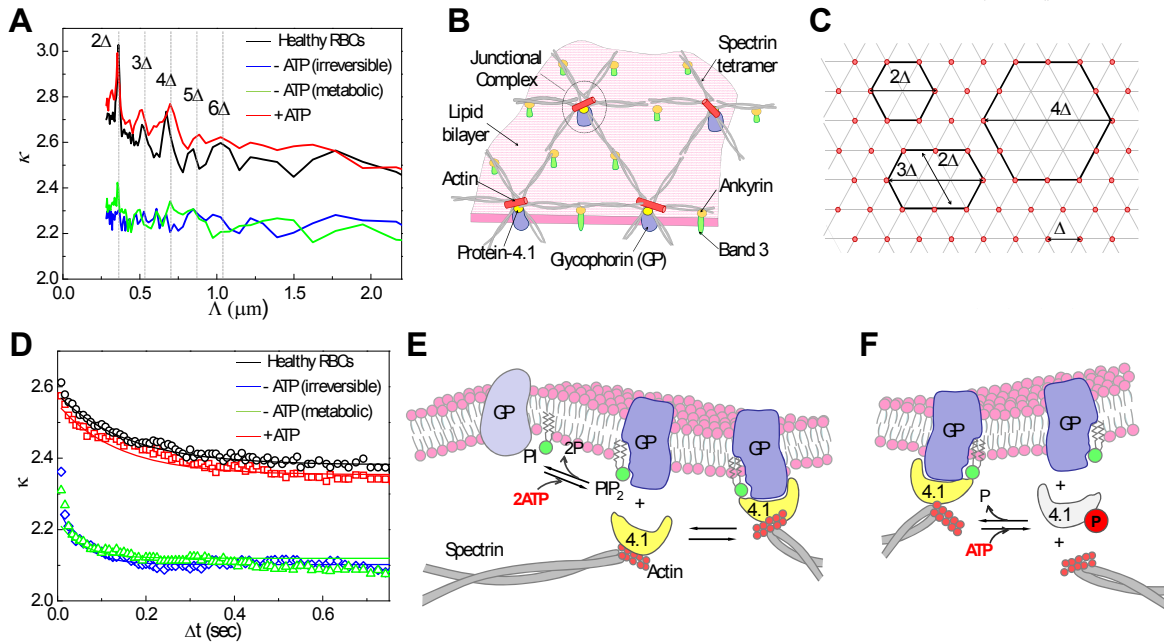


Figure 4. (A), Non-Gaussian parameter at short time delay ( $\Delta t < 0.1$  sec) as a function of spatial wavelength. The presence of ATP lead to non-thermal fluctuations, especially at  $\Lambda=361, 512, 680, 860,$  and  $1030$  nm. (B), Illustration showing the major proteins in the anchor complexes and the spectrin network. (D), Non-Gaussian parameter at spatial wavelength ( $q=15$  rad/ $\mu\text{m}$ ) as a function of a lag time. (E-F), models explaining the non-equilibrium dynamics in RBC membranes by phosphorylation of PI (E) and by phosphorylation of protein-4.1 (F). Reprinted from Ref. [27]. Copyright (2010) National Academy of Sciences, USA

### 3.5 Dynamic remodeling in RBC membrane cortex

The question then arises, how can ATP cause this dynamic remodeling of the cytoskeletal attachment? This may be related to protein phosphorylation powered by ATP, which is one of the physiological processes that control membrane stability. One possible candidate is the phosphorylation of the phosphoinositides (PI) because it consumes more ATP than the combined phosphorylation of all the membrane proteins [32].  $\text{PIP}_2$ , phosphorylated from PI by ATP, is thought to play an important role in modulating the binding of the lipid bilayer to the cytoskeleton by altering the protein interactions that comprise the junctional complex at spectrin tetramer ends [33]. For example,  $\text{PIP}_2$  strengthens the binding affinity of protein-4.1 to glycophorin C (GP) [34] (Fig. 4e). Furthermore,  $\text{PIP}_2$  dephosphorylation results in a decreased affinity for GP binding, and a subsequent detachment from spectrin network; the latter can result in increased membrane fluctuations since tension applied to the bilayer by spectrin network is locally and transiently released. In the absence of ATP, this dynamic remodeling may not occur, and thus RBCs exhibit only thermally driven membrane fluctuations. Another possibility is the phosphorylation of protein-4.1, which results in a reduced binding affinity between the actin, protein-4.1, and GP at the junction [35] (Fig. 4f).

The phosphorylation-dependent binding of the cytoskeleton to the membrane can also explain the correlation between nonequilibrium dynamic fluctuations and biconcave shape. Several models have been proposed to explain the biconcave shape of RBC [36], but it still remains as an unsolved puzzle. It was proposed that the ATP-regulated interactions between the junction complex and the membrane plays a role in maintaining the biconcave shape [34]. A theoretical model, which relates ATP-induced unbinding to RBC shape, showed that this active process lowers the overall cytoskeleton shear rigidity and the tension that the spectrin network imposes on the membrane [16, 37]. Our results provide further experimental evidence for the metabolism-dependent shape transformation; we show that ATP-dependent transient binding of junctional complexes are localized over the cell outer area, and that the spectrin network should therefore exert a lower tension on the membrane. We also note that in the absence of ATP, the shapes of RBC are similar to those of patients with hereditary elliptocytosis, where GP does not properly interact with protein 4.1, resulting

in the lack of biconcave shape and deformability [38, 39]. This dynamic remodeling of the spectrin network also offers a possible explanation for the observed metabolic dependence of red cell deformability [40]. Taken together, we have shown that the biconcave shape and nonequilibrium dynamics in the membrane are both consequences of the same biochemical activity: the dissociations of the cytoskeleton at the spectrin junctions, powered by ATP metabolism.

#### 4. CONCLUSION & FUTURE WORK

We have presented definitive evidence that membrane fluctuations in the RBC membrane have a metabolic as well as thermal energy component, which are localized at the outer area of the cell. Our results suggest that the dynamics of spectrin-bilayer binding, through local remodeling of the spectrin junctions, gives rise to this nonequilibrium dynamics. This same remodeling activity is also important in determining cell deformability and the unique biconcave shape of RBCs. Our results are in good qualitative agreement with previously proposed theoretical models [16, 37]. The values measured for the ATP-mediated fluctuation amplitudes, which are lower than those predicted theoretically, can be understood by the spatial inhomogeneity of active motions.

Further instrumentation development may enable us to understand the more detailed mechanism of metabolic remodeling of the RBC membrane dynamics. Recently, we have employed a Fourier transform light scattering (FTLS) technique and showed that the RBC static and dynamic scattering signals are altered by adenosine 5'-triphosphate (ATP)-driven membrane metabolic remodeling [41]. Simultaneous measurement of mean cellular volume and mean corpuscular hemoglobin concentration on top of the dynamic membrane fluctuation signal may also provide insight into the non-equilibrium in detail. Single molecule technique such as Förster resonance energy transfer (FRET) or super resolution imaging techniques can be used to further study the role of the junctional protein complex in the metabolic remodeling of RBC membrane. Exploring the non-equilibrium dynamics in general eukaryotic cell membrane will be an interesting topic to be explored. Whether this dynamic remodeling of the RBC cytoskeleton *in-vivo* is beneficial remains an open question, and is now accessible to direct experimental study. In addition, the non-equilibrium dynamics measured by diffraction phase microscopy can guide theory [37, 42] and computational simulations that address a broader range of problems concerning soft matter physics, cell pathophysiology, and drug efficacy assays.

#### REFERENCES

- [1] N. Mohandas, and E. Evans, "Mechanical Properties of the Red Cell Membrane in Relation to Molecular Structure and Genetic Defects," *Annual Reviews in Biophysics and Biomolecular Structure*, 23(1), 787-818 (1994).
- [2] F. Brochard, and J. F. Lennon, "Frequency spectrum of the flicker phenomenon in erythrocytes," *J. Physique*, 36, 1035-1047 (1975).
- [3] A. Zilker, H. Engelhardt, and E. Sackmann, "Dynamic reflection interference contrast (RIC-) microscopy: a new method to study surface excitations of cells and to measure membrane bending elastic moduli," *J. Physique*, 48, 2139-2151 (1987).
- [4] N. Gov, A. G. Zilman, and S. Safran, "Cytoskeleton Confinement and Tension of Red Blood Cell Membranes," *Phys. Rev. Lett.*, 90(22), 228101 (2003).
- [5] G. Popescu, T. Ikeda, K. Goda *et al.*, "Optical Measurement of Cell Membrane Tension," *Phys. Rev. Lett.*, 97(21), 218101 (2006).
- [6] G. Popescu, Y. K. Park, R. R. Dasari *et al.*, "Coherence properties of red blood cell membrane motions," *Phys. Rev. E*, 76(3), 31902 (2007).
- [7] G. Popescu, Y. Park, W. Choi *et al.*, "Imaging red blood cell dynamics by quantitative phase microscopy," *Blood Cells, Molecules, and Diseases*, 41(1), 10-16 (2008).
- [8] M. Costa, I. Ghiran, C. Peng *et al.*, "Complex dynamics of human red blood cell flickering: Alterations with *in vivo* aging," *Physical Review E*, 78(2), 20901 (2008).
- [9] D. Szekely, T. Yau, and P. Kuchel, "Human erythrocyte flickering: temperature, ATP concentration, water transport, and cell aging, plus a computer simulation," *European Biophysics Journal*, 38(7), 923-939 (2009).
- [10] T. Betz, M. Lenz, J. Joanny *et al.*, "ATP-dependent mechanics of red blood cells," *Proc. Natl. Acad. Sci. U. S. A.*, 106(36), 15312-15317 (2009).

- [11] B. Rappaz, A. Barbul, A. Hoffmann *et al.*, “Spatial analysis of erythrocyte membrane fluctuations by digital holographic microscopy,” *Blood Cells, Molecules, and Diseases*, 42(3), 228-232 (2009).
- [12] Y. Park, C. Best, K. Badizadegan *et al.*, “Measurement of red blood cell mechanics during morphological changes,” *Proceedings of the National Academy of Sciences*, 107(15), 6731 (2010).
- [13] T. Browicz, “Further observation of motion phenomena on red blood cells in pathological states,” *Zbl. med. Wissen*, 28(1), 625-627 (1890).
- [14] S. Tuvia, S. Levin, A. Bitler *et al.*, “Mechanical fluctuations of the membrane-skeleton are dependent on F-actin ATPase in human erythrocytes,” *J. Cell Biol.*, 141(7), 1551-1561 (1998).
- [15] J. Evans, W. Gratzner, N. Mohandas *et al.*, “Fluctuations of the Red Blood Cell Membrane: Relation to Mechanical Properties and Lack of ATP Dependence,” *Biophysical Journal*, 94(10), 4134 (2008).
- [16] N. S. Gov, and S. A. Safran, “Red Blood Cell Membrane Fluctuations and Shape Controlled by ATP-Induced Cytoskeletal Defects,” *Biophys. J.*, 88(3), 1859 (2005).
- [17] J. Li, G. Lykotrafitis, M. Dao *et al.*, “Cytoskeletal dynamics of human erythrocyte,” *Proc. Natl. Acad. Sci. U. S. A.*, 104(12), 4937 (2007).
- [18] Y. K. Park, G. Popescu, K. Badizadegan *et al.*, “Diffraction phase and fluorescence microscopy,” *Opt. Express*, 14(18), 8263-8268 (2006).
- [19] G. Popescu, T. Ikeda, R. R. Dasari *et al.*, “Diffraction phase microscopy for quantifying cell structure and dynamics,” *Opt. Lett.*, 31(6), 775-777 (2006).
- [20] V. Lew, and H. Ferreira, [Calcium transport and the properties of a calcium-activated potassium channel in red cell membranes] Academic Press, (1978).
- [21] Y. Park, M. Diez-Silva, G. Popescu *et al.*, “Refractive index maps and membrane dynamics of human red blood cells parasitized by *Plasmodium falciparum*,” *Proc. Natl. Acad. Sci. U.S.A.*, 105(37), 13730 (2008).
- [22] D. Fu, W. Choi, Y. Sung *et al.*, “Ultraviolet refractometry using field-based light scattering spectroscopy,” *Optics Express*, 17(21), 18878-18886 (2009).
- [23] Y. Park, T. Yamauchi, W. Choi *et al.*, “Spectroscopic phase microscopy for quantifying hemoglobin concentrations in intact red blood cells,” *Optics Letters*, 34(23), 3668-3670 (2009).
- [24] Y.-K. Park, C. A. Best, and G. Popescu, [Optical sensing of red blood cell dynamics] Springer Science+Business Media, LLC, 13 (in press).
- [25] C. Lawrence, N. Gov, and F. Brown, “Nonequilibrium membrane fluctuations driven by active proteins,” *The Journal of Chemical Physics*, 124(7), 074903 (2006).
- [26] M. Sheetz, and S. Singer, “On the mechanism of ATP-induced shape changes in human erythrocyte membranes. I. The role of the spectrin complex,” *Journal of Cell Biology*, 73(3), 638-646 (1977).
- [27] Y. K. Park, C. A. Best, T. Auth *et al.*, “Metabolic remodeling of the human red blood cell membrane,” *Proc. Nat. Acad. Sci.*, 107, 1289 (2010).
- [28] T. Auth, S. Safran, and N. Gov, “Fluctuations of coupled fluid and solid membranes with application to red blood cells,” *Physical Review E*, 76(5), 51910 (2007).
- [29] S. Tuvia, A. Almagor, A. Bitler *et al.*, “Cell membrane fluctuations are regulated by medium macroviscosity: Evidence for a metabolic driving force,” *Proc. Natl. Acad. Sci. U. S. A.*, 94(10), 5045-5049 (1997).
- [30] D. Mizuno, C. Tardin, C. Schmidt *et al.*, “Nonequilibrium Mechanics of Active Cytoskeletal Networks,” *Science*, 315(5810), 370 (2007).
- [31] F. Liu, H. Mizukami, S. Sarnaik *et al.*, “Calcium-dependent human erythrocyte cytoskeleton stability analysis through atomic force microscopy,” *Journal of Structural Biology*, 150(2), 200-210 (2005).
- [32] E. Muller, H. Hegewald, K. Jaroszewicz *et al.*, “Turnover of phosphomonoester groups and compartmentation of polyphosphoinositides in human erythrocytes,” *Biochemical Journal*, 235(3), 775 (1986).
- [33] V. Patel, and G. Fairbanks, “Spectrin phosphorylation and shape change of human erythrocyte ghosts,” *Journal of Cell Biology*, 88(2), 430-440 (1981).
- [34] P. Agre, and J. Parker, [Red blood cell membranes: structure, function, clinical implications] CRC Press, (1989).
- [35] S. Manno, Y. Takakuwa, and N. Mohandas, “Modulation of erythrocyte membrane mechanical function by protein 4.1 phosphorylation,” *Journal of Biological Chemistry*, 280(9), 7581 (2005).
- [36] E. Beutler, [Williams hematology] McGraw-Hill New York, (1995).
- [37] N. S. Gov, “Active elastic network: Cytoskeleton of the red blood cell,” *Phys.Rev.E*, 75(1), 11921 (2007).
- [38] G. Tchernia, N. Mohandas, and S. Shoet, “Deficiency of skeletal membrane protein band 4.1 in homozygous hereditary elliptocytosis. Implications for erythrocyte membrane stability,” *Journal of Clinical Investigation*, 68(2), 454 (1981).

- [39] S. Suresh, "Mechanical response of human red blood cells in health and disease: some structure-property-function relationships," *J. Mater. Res.*, 21(8), 1872 (2006).
- [40] M. Fred, and M. Pickens, "Metabolic dependence of red cell deformability," *The Journal of Clinical Investigation*, 48, 795 (1969).
- [41] Y. Park, C. Best-Popescu, R. Dasari *et al.*, "Light scattering of human red blood cell during metabolic remodeling of the membrane," *Journal of Biomedical Optics*, 16(1), 011013 (2011).
- [42] E. Ben-Isaac, Y.-K. Park, G. Popescu *et al.*, "Effective Temperature of Red Blood Cell Membrane Fluctuations," *Phys. Rev. Lett.*, (submitted).